Evolution of Moisture and Cloud Distribution during the First Transition of Asian Summer Monsoon

Cheng-Ta Chen[1] and Huang-Hsiung Hsu[2]

[1]National Taiwan Normal University, Dept. of Earth Sciences
[2]National Taiwan University, Dept. of Atmospheric Sciences

Abstract

Composite picture of the evolution of moisture and cloud distribution during the first transition of Asian summer monsoon is constructed based on a corresponding large-scale circulation study and recent compilations of several hydrological datasets. The characteristics of abrupt change in water vapor and cloud fields over the study domain is highlighted. Dry and clear-sky conditions are generally found from 60°E to 140°E and 5°N to 20°N before the first transition of Asian summer monsoon over East Asia, especially over the oceanic regions. It is shown that the dry condition is more due to the dynamical impact on moisture instead of the influence from sea surface temperature. The sudden jump of tropical convective systems from equatorial region to the three oceanic bays over South and East Asia in 2-3 weeks time is clearly depict by the large increase of moisture through the whole tropospheric column and cloud cover at the onset stage. It is not only the cloud fraction raised. The reduction of mean cloud-top pressure, the increase of cloud optical depth, and coherent vertical structure of moistening all demonstrate the focused hydrological changes are of deep convective nature. The arrival of the India summer monsoon with another boost in cloud cover and column moisture over the India subcontinent and eastern Arabian Sea are shown to lag the first transition of Asian summer monsoon over the East Asia about 2-3 weeks. The further reduction in cloud and moisture over the Arabian Peninsula and Iranian Plateau shows the remote linkage between monsoon and desert dynamics. The northward migration of the stationary Mei-Yu frontal system signifies the later monsoonal development in East Asia can be traced by the zone of positive cloud anomalies extended from the Yangtze river valley to south of Japan. These frontal cloud system with the support of the moisture transport from south reveals a more convective nature than that before thetransition through the reduction of the partition of low cloud in total cloud fraction.

1. INTRODUCTION

The development of the Asian Summer Monsoon has been shown to have two distinct transitional periods (He et al.,1987; Yanai et al., 1992). The first transition accompanied by an abrupt changes in the low-level wind direction, convective activity, and the upper tropospheric temperature and upper-level anti-cyclonic circulation over Bay of Bengal and South China Sea. These features normally occurred in the mid-May. The second transition corresponds to the establishment of the Indian summer monsoon usually comes around early to mid-June. There are quite a few studies focused on the Indian summer monsoon and its onset (Ramage, 1971; Lighthill and Pearce, 1981; Chang and Krishnamurti, 1987). Relatively less efforts are put in the study of the first transition period or the onset of summer monsoon over East Asia (Lau and Li, 1984; Chen et al., 1991; Yanai et al., 1992). The complex of the first transition and its relationship to the other components of Asian Monsoon System has been illustrated in Fig. 3.8 in Tao and Chen (1987). The influences from the Mei-Yu front and mid-latitude synoptic scale disturbance (Chang and Chen, 1995), the location and strength of the subtropical high in the western Pacific, the cross-equatorial flow (Tao and Chen, 1987), the interaction with the tropical intraseasonal oscillation (Krishnamurti and Bhalme, 1976; Yasunari, 1980; Lau and Chan, 1986; Chen and Chen, 1995), and lower boundary forcing (Krishnamurti and Ramanathan, 1982; He et al., 1987; Hsu et al, 1998) all seem to play a role in forming the seasonal abrupt change in the dynamical and thermodynamical fields over the East Asia. Due to these complex factors, this first transitional period is expected to have considerable interannual variability, especially due to the influence from the ENSO events (Rasmusson and Crapente, 1983; Webster and Yang, 1992). In a related sequential study by Hsu et al. (1998), a conceptual model has been built to highlight the climatological mean evolution of these different elements and their interactions using a composite technique. Here we provide supplements to the previous picture by examining the hydrological fields using recent compilations of water vapor and cloud climatologies.

Conventional meteorological information, including station and analyses data, are normally used the previous Monsoon observational studies. Here we offer further information mostly from the satellite views. The seasonal migration or even abrupt change in the large scale circulation and

* *Corresponding author address*: Dr. Cheng-Ta Chen, National Taiwan Normal University, Department Of Earth Sciences, No. 88, Sec. 4, Ting-Chou Road, Taipei, Taiwan; e-mail: chen@cloud.geos.ntnu.edu.tw

the associated convective activity are one of the main characteristics of the establishment and development of the monsoon. The local changes in moisture and cloud fields are expected and can be traced by the satellite with unprecedented spatial and temporal coverage. The purpose of this study is to draw a more complete picture of the changes in the hydrological components of the atmosphere during the first transitional period of Asian Summer Monsoon.

2. DATA SETS

2.1 *NASA Water Vapor Project*

A 5-year (1988-1992) total and layered global water vapor data set has been produced by NASA Water Vapor Project (NVAP, Randel et al., 1996). Single water vapor measuring system usually has limitation on accuracy in specific situation and/or areas. Radiosonde data is mainly over land and too sparse to resolve smaller scale moisture fluctuation for some region. Furthermore, the radiosonde data is less reliable in the upper troposphere. Infrared satellite retrieval method can not be used in cloudy regions, therefore tend to have dry sampling bias. Microwave data is not retrieved over land and sea ice due to the large variation in surface emissivity. NVAP combined the radiosonde observation, TIROS Operational Vertical Sounder (TOVS), and Special Sensor Microwave/Imager (SSM/I) data sets together to form a merged product. A weighting scheme is used when more than one input data sets are merged. The accuracy factor for each measuring system determines the weighting of data for coincident points. The more detailed information on the different measuring systems and error analyses can be found in the previous studies (Gaffen et. al. 1991; Wu et al., 1993; Liu et al., 1992; Soden and Lanzante, 1996). A quality control procedure is applied to NVAP data for minimizing the impact from the possible problem areas and false values.

The data set have a daily time scale and $1^{\circ} \times 1^{\circ}$ resolution. The 5 years period of data is shorter than the other analyzed fields in a related study by Hsu et al. (1998). However, it still should be representable for the climatological mean condition for the variations of moisture fields in the chosen transitional time frame of the East Asian Summer Monsoon. Although daily data are provided, we use only the pentad average of total column integrated moisture amount. The intention is to describe only the significant change during different stages of the transitional period of the Asian Summer Monsoon. The key pentad for the monsoon onset in different years follows the description in Hsu et al. (1998, see Table 1). Composite pictures are then formed by taking the ensemblepentad mean fields for the 5 year period. Due to the shorter time span of this data set as compared to the analyses data used to describe the large-scale circulation features, one should note that the interannual variability in moisture distribution might influence the composite picture. However, we intent to only highlight the climatological aspect using the newly merged data set with global coverage. The analyzed domain is restricted to between 30°E and 180°E, and between Equator and 45°N.

Table 1. Occurring dates of the first transition of Asian Summer Monsoon (from Table 1, Hsu et al. (1987))

Year	Date	Year	Date	Year	Date
1979	5/18	1984	5/28	1989	5/23
1980	5/18	1985	5/28	1990	5/18
1981	5/10	1986	5/11	1991	6/7
1982	5/28	1987	5/31	1992	5/18
1983	5/28	1988	5/13	1993	5/28

2.2 *International Satellite Cloud Climatology Project*

International Satellite Cloud Climatology Project (ISCCP) The related cloud fields examined in this study are mostly derived from the C1 dataset produced by ISCCP. A detailed description of the ISCCP data processing and products is given by Rossow and Schiffer (1991). The analyzed visible and thermal infrared radiances from the NOAA Polar Orbiting Satellites, and GOES, GMS, and METEOSAT Geostationary Satellites are first sampled at 30 km and three-hourly resolution and normalized in calibration by reference to the NOAA-7 Advanced Very High Resolution Radiometer (AVHRR) to form the ISCCP-B3 data. Then these data are merged at 280 km resolution to become the ISCCP-C1 data. The cloud analyses procedures include cloud detection, radiative model and statistical analysis. Calibration and adjustment procedures are used in various stages to improve the quality of the monitoring. The uncertainty of the cloud detection scheme is judged to be about 10-15% (Rossow and Lacis, 1990). The estimated random errors for cloud optical thickness and cloud-top altitude are 2 and 0.5 km, respectively (Rossow and Lacis, 1990). Among the 132 cloud parameters in the C1 dataset, we focus our attention on the spatial and temporal evolution of the grid-averaged cloud fraction, cloud-top pressure, and cloud optical thickness. Table 2 shows the cloud types assigned to the cloudy pixels. The analyzed cloud-top pressure and the cloud optical thickness at each pixel are used for the cloud type classification. Instead of the conventional descriptive name (Rossow and Schiffer, 1991), the cloud-top pressure and optical thickness are used directly to refer the cloud type (Lau and Crane, 1995). The above nephanalyses provide a more detailed statistics on the distribution of cloud-top height and cloud thickness when cloud occur during the study period.

Table 2. Cloud type classification according to cloud-top pressure (mb) and cloud optical depth

	cloud-top pressure	Cloud optical depth			
		0-3.6	3.6-9.4	9.4-23	23-125
High top	50-310	high top/ thin		high top/ medium	high top/ thick
	310-440				
Mid-top	440-680	mid-top/ thin		mid-top/ thick	
Low top	680-1000	low top/ thin	low top/ thick		

The ISCCP equal area cells are then transferred to an array with 2.5° grid interval in latitude and longitude. Available C1 data for the period from 1984 to 1990 are used for this study. This period is again shorter than the analyzed

fields in the first part of this study and also different from that for the moisture information described above. However, the 7 year length should be representable for the climatological mean condition of the variations of cloud fields in the chosen time frame of the East Asian Summer Monsoon transition. Although the cloud analyses are generated up to every three hours, we use only the pentad average of cloud parameters. A similar procedure to construct the composite picture based on the onset dates in the different years as described in previous subsection is also applied here.

3. MOISTURE FIELDS

The pattern of water vapor changes with the temporal changes in temperature distribution and atmospheric circulation. Using the NASA NVAP data and the summer monsoon transition information from Hsu et al. (1998), the time-mean water vapor distribution, its pre-onset, onset, and post-onset anomalies are highlighted. The moisture changes in different tropospheric vertical layers is also discussed. The time mean vapor distribution from the examined transitional period is taken from 9 pentads centered at the chosen key-date. The pre-onset, onset, and post-onset anomalies are moisture amount deviation from the mean in the -4, 0, and +4 pentad, respectively.

3.1 *Mean in transitional period*

The geographic distribution of 5 year ensemble period mean total precipitable water (hereinafter TPW) is shown in Fig. 1a. The strong influence from the seasonal temperature distribution on the column integrated moisture can be clearly seen in the meridional TPW gradient. This is especially true for the mid-latitude western Pacific region. Large TPW (>45 Kg/m^2) are found in most of the equatorial region of the study area. The maximum TPW during the period are located in the Intertropical Convergent Zone (ITCZ), southern Philippines and the Andaman Sea. The close relationship between sea surface temperature and TPW can be expected from thermodynamic link (Stephens et al., 1990). The TPW over land is more complicated due to the topography, soil, or even vegetation. Topographic impact on column moisture is evident over the Tibetan Plateau. Besides the thermodynamic effect, we use the normalized TPW parameter following the work by Stephens et al. (1990) to highlight the dynamical impact on the TPW. The normalized TPW parameter, TPW*, is defined as follows:

$$TPW^* = \frac{(TPW - TPW')}{TPW} \qquad (1)$$

TPW$'$ in (1) is the total precipitable water estimated using a simplified model based on an approximate version of the Clausius-Clapeyron equation:

$$TPW' = 10.82\frac{r}{(1+\lambda)}exp(0.064(T_s - 288)) \qquad (2)$$

where T_s is the sea surface temperature (SST), r is the relative humidity and l is the ratio of the atmospheric scale height to the scale height of water vapor and has a typical value of 3.5. The factor $\frac{r}{(1+\lambda)}$=0.165 is determined following Soden and Bretherton (1994) by using a regression between TPW from SSM/I and the right hand side of (2) using the monthly SST climatology from Reynolds and Smith (1995). The positive TPW* means a greater than average TPW for a specific SST. Thus, it is likely to be located in regions with moisture convergence or moist advection. The negative value, on the other hand, suggest the influence of subsidence or dry air advection. The averaged dynamical effects during the 9-pentad study period are clearly illustrated(not shown). Due to the use of SST, only oceanic areas are analyzed. The subsidence over the subtropical high in the western Pacific leads to small negative TPW*. Large negative TPW* over the northern Arabian Sea is due to both the dry air advection from the surrounding land masses and subtropical air descent. The positive TPW* reflecting the moisture convergence in the ITCZ and maritime continent. The relative moist air over the North Pacific is also consistent with the large northward flux of moisture by transient eddies.

3.2 *Anomalies in Pre-onset, Onset, and Post-onset*

The ensemble mean TPW anomalies in the pre-onset (-4 pentad), onset (0 pentad), and post-onset (+4 pentad) are shown in Fig. 1b-1d, respectively. In the pre-onset stage, there are relatively dry air in the South China Sea, Bay of

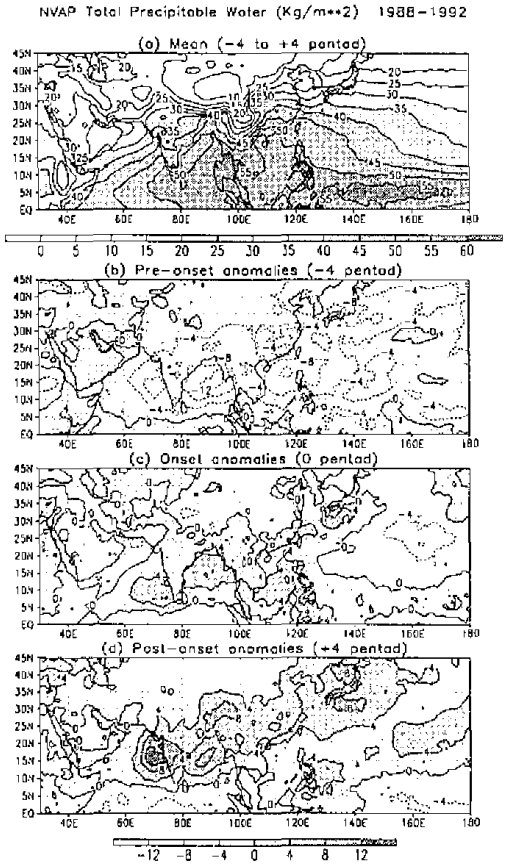

Fig. 1 Geographic distribution of the (a) 9-pentad mean, (b) pre-onset anomalies, (c) onset anomalies, and (d) post-onset anomalies for the NVAP total precipitable water. The pre-onset, onset, post-onset stages are represented by the -4, 0, and +4 pentad mean value centered at the chosen onset dates. Units are kg/m^2

Bengal and Arabian Sea. Few convective activities and the accompanied moisture convergence occurred in these regions before the first transition of Asian Summer Monsoon. The dynamical processes, revealed by TPW^*, tends to reduce the water vapor amount for most of the study area, especially in the three oceanic regions in the South Asia along the 10-20°N belt. The TPW over Arabian Peninsula and East Africa are actually more abundant at this stage (Fig. 1b). When the abrupt transition of the summer monsoon comes, the sudden increases of TPW over the three oceanic bays are evident (Fig. 1c). Moreover, the column vapor amount over the ITCZ and Mei-Yu frontal system are also increase at the transition pentad. The anomalous dry subtropical Pacific depicts the retreat of the high pressure system from the South Asia. One can find a complete reversed dynamical impacts over the regions with increase in TPW. Four pentad after the first transition, one of the major changes from the first transition is the sharp increase of TPW over the west of Indian subcontinent (Fig. 1d). It corresponds well to the establishment of the Indian Summer Monsoon. There are also large increases in TPW over the mid-latitude. However, they are partly due to the temperature change during the seasonal transition. Nevertheless, the increases in TPW over Japan and surrounding region are indeed affected by the dynamical processes. The northward shift of the Mei-Yu frontal system are likely to explain the enhanced dynamical effect. Another notable change is the absence of the negative TPW^* over subtropical Pacific high.

4. CLOUD FIELDS

Cloud formation closely relates to the distribution, transport, and convergence of moisture. The relative humidity and dynamical processes provide the linkage between moisture and liquid water in the atmosphere. Conversion between water vapor and cloud also points to the latent heat release which is the major physical mechanism to balance the radiative cooling in the atmosphere. Cloud itself also plays a decisive role in the radiative transfer in the earth-atmosphere system. Thus, the changes in cloud fields not only reveal the transition of the large-scale circulation but also the differences in the energy distribution during the study period. It is of interest to further show the corresponding climatological evolution of the cloud fields and compare the results to those of the moisture field. Among many cloud parameters available in the ISCCP C1 dataset, only a few most relevant cloud fields are shown. Since ISCCP data provides an unprecedented long-term cloud-type climatology based on the satellite-derived cloud-top pressure and cloud optical depth, it is of importance to also illustrate these rich informations beyond only the total cloud fraction. For the sake of comparison, we process the data using the same procedure to decide the onset dates and transitional period of the Asian summer monsoon as in the previous section. A 7-year (1984-1990) cloud climatology is used. Although the period is not overlapped with the moisture data from NVAP, the intention here is to provide the description of changes in cloud fields from a climatological view. With the help of a systematic way to choose the onset dates in different years, one actually minimizing the inter-annual variability on the seasonal timing of first transition of the Asian summer monsoon. Actually the results do not alter significantly even if we applied the same analyses for the overlapped three years (1988-1990). The anomalous fields in the -4, 0, and +4 pentad with respect to the key onset dates are again referred to the deviations in the pre-onset, onset, and post-onset stages from the total 9-pentad mean value, respectively.

4.1 *Fractional total cloud cover*

Over 80% mean cloud cover is found in the Bay of Bengal and eastern Indian Ocean during the transition period (Fig. 2a). Other area with large and persistent cloud cover is over the storm track in the mid-latitude western Pacific. In additional to the frequent convective activities and large cloud fraction in the ITCZ, the stationary frontal system found in the southeastern China also leads to relatively larger mean cloud amount. On the other hand, small cloud amounts are presented over the subtropical high in the western Pacific and the dry desert zone over Arabian Peninsula and Northern Africa. Fig. 2b-2d show the anomalous total cloud fraction at -4, 0, and +4 pentad as compared to

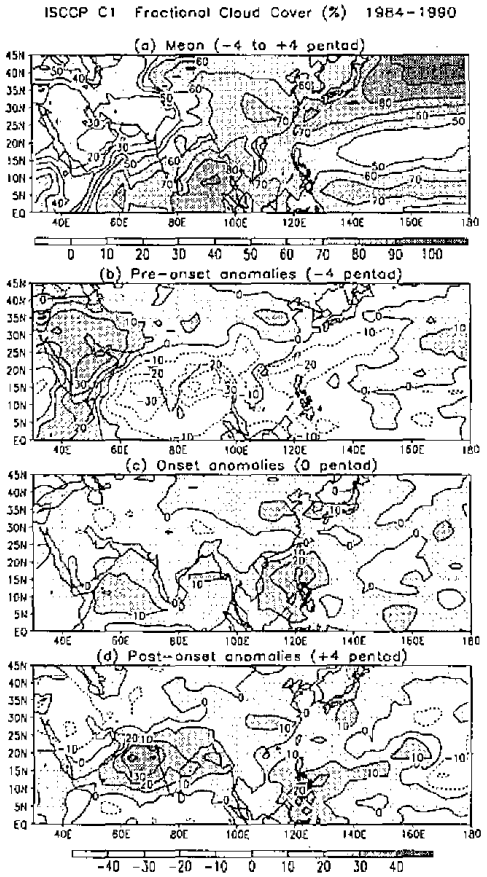

Fig.2 Geographic distribution of the (a) 9-pentad mean, (b) pre-onset anomalies, (c) onset anomalies, and (d) post-onset anomalies for the ISCCP total fractional cloud cover. The pre-onset, onset, post-onset stages are represented by the -4, 0, and +4 pentad mean value centered at the chosen onset dates. Units are %.

the mean total cloud cover of the 9 pentad studied. Prior to the first transition of summer monsoon in the East Asia, large negative cloud anomalies indicate a relatively stable conditions over the Arabian Sea, Bay of Bengal, and South China Sea (Fig. 2b). The negative anomalous cloudiness in the South China Sea at the pre-onset stage actually extend northeastward to the southeast of Japan. It suggests the spatial extent of the subtropical high are more toward the west before the abrupt change in circulation and thermal fields over East Asia. The total cloud fraction over the Arabian Peninsula at this stage is much higher than the later period.

In contrast to the largest positive moisture anomalies in the Bay of Bengal in the onset pentad, the largest positive cloud cover anomalies are in the South China Sea and Philippine (Fig. 2c). However, this contrast may be in part due to the large mean cloud cover over the Bay of Bengal in limiting further increases in cloudiness. There are nearly overcast conditions over the three oceanic bays in the south Asia at the chosen onset pentad. The arrival of South Asian (Indian) summer monsoon is clearly depicted by the large increase of the total cloud amount in Arabian Sea and Indian subcontinent 4 pentads after the onset of East Asian summer monsoon (Fig. 2d). It is consistent with the northward shift and intensification of low-level southwesterlies (Hsu et al., 1998). The cloud fraction in the South China Sea and Philippine remains large in the post-onset stage. The positive anomalous cloudiness in the Yangtze river valley and south of Japan are corresponding to the northward advance of the stationary frontal cloud system. While there is generally large cloud fraction in the east and south Asia, almost no cloud is found in the Arabian Peninsula.

4.2 *Mean cloud top pressure*

Another useful information is the cloud top pressure retrieved from the satellite data. The mean cloud top pressure, averaged from individual cloudy pixel, is an estimate of the overall vertical development of a cloud system at different transitional stages. Fig. 3a shows the geographic distribution of the mean cloud top pressure for the study period.Although the mean cloudiness are large in both the Bay of Bengal and mid-latitude storm track (Fig. 2a), it is clearly that the cloud top altitudes associated with the tropical convective system over the Bay of Bengal are higher than those associated with the mid-latitude baroclinic activities. Mean cloud top pressure over the ITCZ and China are also relatively small. On the other hand, the mean cloud top pressure is larger over northern Arabian Sea, Persian Gulf, and Pakistan. One also expects to fin the lower cloud top over the subsiding region of subtropical high in the Pacific. For the anomalous mean cloud top pressure at the pre-onset stage, it is interesting to note that not only there are fewer cloudiness over Arabian Sea, Bay of Bengal, South China Sea and western Pacific. They also in general have lower mean cloud top height when cloud presents during this period (Fig. 3b). Similarly, the more-than-average cloudiness over the Arabian Peninsula accompanies higher mean cloud top height before the summer monsoon transition occurs. The increased convective strength in cloud systems over the three oceanic bays regions after the chosen onset dates is clearly depicted by the further reduction in cloud top pressure. There is again opposite trend in the anomalous cloudiness and cloud top height at the onset pentad, especially over the Philippine and surrounding ocean (Fig. 3c). The arrival of Indian summer monsoon at the post-onset stage (+4 pentad) not only greatly increase the over the northern Arabian Sea and Bay of Bengal but also rise the cloud top height through much organized convective cloud system of the monsoon depression (Fig. 3d). The tropical and subtropical cloud over the East Asia and Western Pacific also show higher extent in the vertical development.

4.3 *Mean cloud optical depth*

ISCCP data provide cloud optical depth information based on the visible reflectance. It links to the abundance of cloud water when cloud presents and reveals the shortwave radiative impact of cloud system. The area with maximum mean cloud optical depth is extended from Central China to the storm track region over Northern Pacific. On average, the tropical cloud band has a smaller water density. Although the deep convective centers tend to have larger water density than other cloud system, much larger tropical regions is covered by the high-level anvil cloud and cirrus associated with the deep convection. Therefore, the aver-

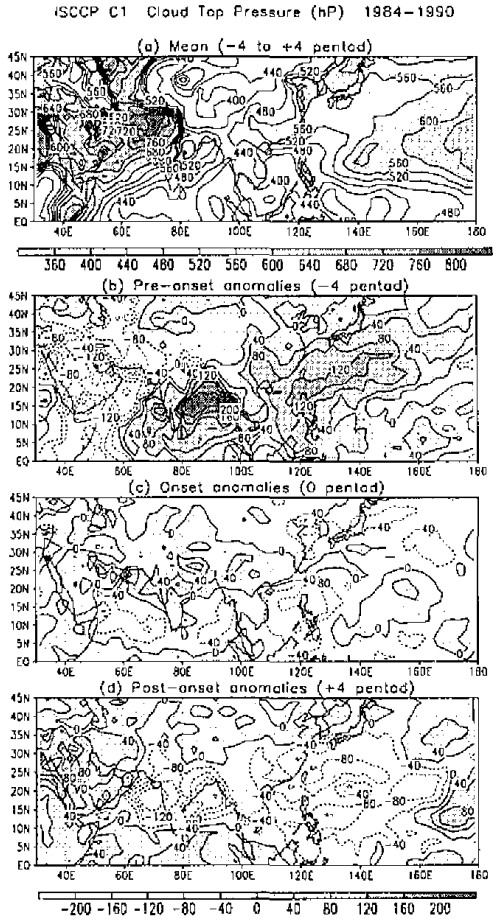

Fig. 3 As in Fig. 2, except for the mean cloud top pressure. Units are hPa

aged cloud optical depth in the tropics is less than that in the mid-latitude cyclonic storm systems. The relatively cloud-free areas over the subtropical western Pacific and Arabian Peninsula during the study period are accompanied with very small cloud optical depth averaged over the 9 pentad period. In additional to fewer cloudiness and lower cloud top, clouds over the three oceanic bays in South and South-east Asia also tend to has smaller optical depth in the pre-onset stage, especially over the Bay of Bengal. During the first summer monsoon transition in East Asia, the cloud water densities increase significantly over the South China Sea and the eastern China. The arrival of Indian summer monsoon after the transition occurred in the East Asia not only bring up the cloud optical depth over the Arabian Sea off east coast of Indian subcontinent, the cloud water densities over the Bay of Bengal (Monsoon depression active region), Indochina Peninsula, and southern Philippine are also increases. The pattern of mean cloud optical depth increase indicates a planetary scale change in physical processes regulate the cloud water density in cloud system.

Acknowledgements

The ISCCP datasets are produced through an effort led by W. B. Rossow at the NASA Goddard Institute of Space Studies. The further processed data tapes have been provided to us by Mr. Mark W. Crane at the NOAA Geophysical Fluid Dynamics Laboratory. The SSM/I cloud water data is kindly provided by Dr. Fuzhong Weng. NASA water vapor project dataset is produced by STC-METSAT and provided by the Marshall Space Flight Center Distributed Active Archive Center (MSFC DAAC). We are grateful to Dr. Brian Soden at the NOAA Geophysical Fluid Dynamics Laboratory for providing the radiance-transformed layer-average relative humidity datasets. The GPCP dataset was provided through World Data Center A. This work is supported by the National Science Council of Taiwan under grant NSC 87-2621-P-003-001, NSC 87-2111-M-003-001-AGT, and NSC 88-2111-M-003-001-AGT.

5. REFERENCE

Chang, C.-P., and G. T.-J. Chen, 1995: Tropical circulation associated with southwest monsoon onset and westerly surges over the South China Sea, Mon. Wea. Rev., 123, 3254-3267.

Chang, C.-P., and T. N. Krishnamurti, Eds., 1987: Monsoon Meteorology, Oxford university press, New York, 544 pp.

Chen, T.-C., and J.-M. Chen, 1995: An observational study of South China Sea monsoon during the 1979 summer: Onset and life cycle. Mon. Wea. Rev., 123, 2295-2315.

Gaffen, D. J., T. P. Barnett, and W. P. Elliot, 1991: Space and time scales of global tropospheric moisture. J. Climate, 4, 989-1008.

Greenwald, T. J., G. L. Stephens, and T. H. Vonder Haar, 1993: A physical retrieval of cloud liquid water over the global oceans using special sensor microwave/imager (SSM/I) observation, J. Geophys. Res., 98, 18471-18488.

He, H., J. W. McGinnis, Z. Song, and M. Tanai, 1987: Onset of the Asian monsoon in 1979 and the effect of the Tibetan Plateau. Mon. Wea. Rev., 115, 1966-1995.

Hsu, H.-H., T.-C. Terng and C.-T. Chen, 1998: Evolution of large-scale circulation and heating during the first transition of Asian summer monsoon. In press, J. Climate.

Krishnamurti, T. N., and H. H. Bhalme, 1976: Oscillation od a monsoon system. Part I: Observational aspects, J. Atmos. Sci., 33, 1937-1954.

Krishnamurti, T. N., and Y. Ramanathan, 1982: Sensitivity of monsoon onset to differential heating. J. Atmos. Sci., 39, 1290-1306.

Lau, K.-M., and P. H. Chan, 1986: Aspects of the 40-50 day oscillation during the northern summer as inferred from outgoing longwave radiation. Mon. Wea. Rev., 114, 1354-1367.

Lau, K.-M., and M. T. Li, 1984: the monsoon of east Asia and its global associations - A survey. Bull. Am. Meteor. Soc., 65, 114-125.

Lau, K.-M. and S. Yang, 1996: Seasonal variation, sbrupt transition, and intraseasonal variability associated with the Asian summer monsoon in the GLA GCM. J. Climate, 9, 965-985.

Lau, N.-C., and M. W. Crane, 1995: A satellite view of the synoptic-scale organization of cloud cover in midlatitude and tropical circulation systems, Mon. Wea. Rev., 103, 1984-2006.

Lighthill, J. and R. P. Pearce, Eds., 1981: Monsoon dynamics, Cambridge university press, Cambridge, 540pp.

Liu, T. W., W. Tang, and F. Wentz, 1992: Precipitable water and surface humidity over global oceans for the SSM/I and ECMWF, J. Geophys. Res., 97, 2251-2264.

Ramage, C. S., 1971: Monsoon Meteorology, Academic Press, New York, 296pp.

Randel, D. L., T. H. Vonder Haar, M. A. Ringerud, G. L. Stephens, T. J. Greenwald, and C. L. Combs, 1996: A new global water vapor dataset, Bull. Amer. Meteor. Soc., 77, 1233-1246.

Rasmusson, E. M., and T. H. Carpenter, T. H., 1983: The relationship between eastern Pacific sea surface temperature and rainfall over India and Sri Lanka, Mon. Wea. Rev., 111, 354-384.

Reynolds, R. W., and T. M. Smith, 1995: A high-resolution global sea surface temperature climatology. J. Climate, 8, 1571-1583.

Rossow, W. B., 1993: Clouds, in Atlas of satellite observations related to global change, R. J. Gurney, J. L. Foster, and C. L. Parkinson (Eds.), Cambridge University Press, Cambridge, UK.

Rossow, W. B. and A. A. Lacis, 1990: Global, seasonal cloud variation from satellite radiance measurements. part II: cloud properties and radiative effects, J. Climate, 3, 1204-1253.

Rossow, W. B. and R. A. Schiffer, 1991: ISCCP cloud data products, Bull. Amer. Meteor. Soc., 72, 2-20.

Soden, B. J., and F. P. Bretherton, 1994: Evaluation of water vapor distribution in general circulation models using satellite observation. J. Geophys. Res., 99, 1187-1210.

Soden, B. J. and J. R. Lanzante, 1996: An assessment of satellite and radiosonde climatologies of upper tropospheric water vapor, J. Climate, 9, 1235-1250.

Stephens, G. L., 1990: On the relationship between water vapor over the ocean and sea surface temperature. J. Climate., 3, 634-645.

Tao, S.-Y., and L.-X. Chen, 1987: A review of recent research on th east Asian summer monsoon in China. Monsoon Meteorology, C.-P. Chang and T. N. Krishnamurti, Eds., Oxford university press, New York, 60-92.

Webster, P. J., and S. Yang, 1992: Monsoon and ENSO: Selectively interactive systems, Q. J. R. Meteor. Soc., 118, 877-926.

Wu, X., J. J. Bates, S. J. S. Khalsa, 1993: A climatology of the water vapor band brightness temperatures from NOAA Operational satellites. J. Climate., 6, 1282-1300.

Yanai, M., C. Li, and Z. Song, 1992: Seasonal heating of the Tibetan Plateau and its effects on the evolution of the Asian summer monsoon. J. Meteo. Soc. Japan, 70, 1B, 319-351.

Yasunari, T., 1980: Aquasi-stationary appearance of 30 to 40 day period in the cloudness fluctuations during the summer monsoon over India. J. Meteor. Soc. Japan., 58, 225-229.